Polarization-insensitive optical gain characteristics of highly stacked InAs/GaAs quantum dots

Kita, Takashi
Suwa, Masaya
Kaizu, Toshiyuki
Harada, Yukihiro

(Citation)
Journal of Applied Physics,115:233512-233512

(Issue Date)
2014

(Resource Type)
journal article

(Version)
Version of Record

(URL)
https://hdl.handle.net/20.500.14094/90002574

Polarization-insensitive optical gain characteristics of highly stacked InAs/GaAs quantum dots

Takashi Kita, Masaya Suwa, Toshiyuki Kaizu, and Yukihiro Harada

Citation: Journal of Applied Physics **115**, 233512 (2014); doi: 10.1063/1.4884228
View online: http://dx.doi.org/10.1063/1.4884228
View Table of Contents: http://scitation.aip.org/content/aip/journal/jap/115/23?ver=pdfcov
Published by the AIP Publishing

Polarization-insensitive optical gain characteristics of highly stacked InAs/GaAs quantum dots

Takashi Kita, Masaya Suwa, Toshiyuki Kaizu, and Yukihiro Harada
Department of Electrical and Electronic Engineering, Graduate School of Engineering, Kobe University, 1-1 Rokkodai, Nada, Kobe 657-8501, Japan

(Received 8 April 2014; accepted 7 June 2014; published online 19 June 2014)

The polarized optical gain characteristics of highly stacked InAs/GaAs quantum dots (QDs) with a thin spacer layer fabricated on an n^+-GaAs (001) substrate were studied in the sub-threshold gain region. Using a 4.0-nm-thick spacer layer, we realized an electronically coupled QD superlattice structure along the stacking direction, which enabled the enhancement of the optical gain of the [001] transverse-magnetic (TM) polarization component. We systematically studied the polarized electroluminescence properties of laser devices containing 30 and 40 stacked InAs/GaAs QDs. The net modal gain was analyzed using the Hakki-Paoli method. Owing to the in-plane shape anisotropy of QDs, the polarization sensitivity of the gain depends on the waveguide direction. The gain showing polarization isotropy between the TM and transverse-electric polarization components is high for the [110] waveguide structure, which occurs for higher amounts of stacked QDs. Conversely, the isotropy of the [−110] waveguide is easily achieved even if the stacking is relatively low, although the gain is small. © *2014 AIP Publishing LLC*.
[http://dx.doi.org/10.1063/1.4884228]

I. INTRODUCTION

Self-assembled InAs quantum dots (QDs) have been extensively studied for use in novel optical communication devices such as cooler-less direct modulation lasers, polarization-insensitive semiconductor optical amplifiers (SOAs), and ultrahigh-speed optical switches. InAs QDs are suitable for such device applications because they can operate in the 1.3- and 1.55-μm optical communication bands. In particular, application of SOAs in high-speed, high-capacity optical communication networks has been expected.[1] Waveguide-type optical devices generally used in such networks strongly demand polarization-insensitive operation. However, generally, SOAs containing conventional self-assembled InAs QDs cannot solve the issue of a strong polarization anisotropy as appeared in SOAs using quantum wells,[2] which gives rise to fluctuating output signals. The transverse electric (TE) optical gain is strong even in self-assembled InAs QDs.[3,4] This is due to the flat shape of self-assembled InAs QDs and a strong biaxial compressive strain, which causes the spin quantization to be oriented vertically and makes the heavy-hole transition TE polarized and the light-hole transition transverse magnetic (TM) polarized. Moreover, the biaxial compressive strain significantly pushes the light-hole band with TM gain away from the band edge. In this manner, the TM gain becomes small near the band edge.

By controlling the optical selection rule arising from the valence-band mixing, highly stacked InAs QDs can be realized as three-dimensionally controlled artificial structures. Owing to a strong strain field near the self-assembled InAs QDs, InAs deposited on a thin spacer layer self-assembly forms QDs above the bottom QDs, which enables fabrication of vertically stacked QD structures. Recently, various types of QD structures, such as strain-controlled InAs/GaAs QDs,[5] columnar InAs/GaAs and InAs/InGaAsP QDs,[6–11] and closely stacked InAs/GaAs (Refs. 12–15) and InAs/InGaAlAs QDs (Refs. 16 and 17), have been reported. Wave functions in such effectively tall QDs are delocalized, which causes the valence-band mixing of the heavy- and light-hole states. The lift of the light-hole component is essential to controlling the optical polarization feature.[8,13,14] In contrast to columnar QDs, closely stacked QDs have a moderately thick spacer layer between QD layers, and the coupling strength between electronic states in vertically stacked QDs can be controlled by changing the spacer layer thickness.[17,18] Thus, vertically coupled QDs can form effective electronic states similarly to columnar QDs. Furthermore, the total amount of QD layers used in closely stacked QDs is less than that used in the columnar QDs, which would diminish dislocation generation, to achieve similar optical polarization features. From this perspective, closely stacked QDs are superior to columnar QDs for polarization control.

Generally, closely stacked QDs give rise to a change in the lateral QD dimension with stacking and tend to generate dislocations.[19] To eliminate these, a strain-compensation growth technique has been proposed,[16] in which accumulation of the lattice mismatched strains can be compensated using a pair of oppositely strained materials against the substrate. Without using such a strain compensation technique, we recently succeeded in fabricating closely stacked InAs/GaAs QDs with a high stacking-layer number (SLN).[13–15] Here, the GaAs-spacer-layer thickness was 4 nm, which is expected to be sufficiently thin to form the miniband.[15] Because the critical thickness of InAs showing self-assembled QD formation in the stacked layers is smaller than that in the first layer, reducing the InAs nominal thicknesses in the stacked layers enables highly stacked InAs/GaAs QDs without forming dislocations.

In this work, we fabricated QD-SOA device structures containing 30 and 40 stacked InAs/GaAs QDs fabricated by controlling the nominal InAs thickness of the stacked layers and studied polarization-insensitive properties of the net modal gain using a SOA structure with high-reflection coating. This device structure is identical to a laser device. The net modal gain was analyzed using the Hakki-Paoli method.[20] Because of the in-plane shape anisotropy of the QDs, the polarization sensitivity of the gain depends on the waveguide direction. We discuss the polarization isotropy of the gain obtained from the waveguide structures fabricated along different orientations.

II. GROWTH OF HIGHLY STACKED InAs/GaAs QDs AND DEVICE STRUCTURES

We fabricated QD-SOA device structures including 30 and 40 stacked InAs/GaAs QDs using solid-source molecular beam epitaxy. The device structure was fabricated on a Si-doped n^+-GaAs(001) substrate. After growing a 150-nm-thick buffer layer of n^+-GaAs doped with $2.5 \times 10^{18}\,\mathrm{cm}^{-3}$ of Si, a 1-μm-thick $Al_{0.3}Ga_{0.7}As$ cladding layer doped with $5.0 \times 10^{17}\,\mathrm{cm}^{-3}$ of Si was grown at 550 °C. Then, an active layer comprising the stacked QD layers was grown at 480 °C. The thickness of the single-mode active layer, which comprised GaAs/stacked QD layers/GaAs, was 400 nm. The thicknesses of the GaAs layer were 135.6 and 113.5 nm for 30 and 40 stacked QD layers, respectively. The growth rate and nominal thickness of the deposited InAs were 0.04 monolayer per second (ML/s) and 2.0 MLs, respectively, for the first QD layer. A 4.0-nm-thick GaAs spacer layer was deposited with a growth rate of 0.8 ML/s. A growth interruption of 10 s was introduced after growing the GaAs spacer layer. Then, the subsequent InAs QD layers with a reduced thickness of 1.4 MLs were alternately formed on the GaAs spacer layer. A Be-doped p^+-$Al_{0.3}Ga_{0.7}As(1.0 \times 10^{18}\,\mathrm{cm}^{-3})$/$p$-$Al_{0.3}Ga_{0.7}As(2.0 \times 10^{17}\,\mathrm{cm}^{-3})$ cladding layer was grown at 500 °C. The thickness of this upper cladding layer was 1 μm. Finally, a thin, p^+-GaAs contact layer doped with $1.3 \times 10^{19}\,\mathrm{cm}^{-3}$ of Be was deposited. Furthermore, we provided a reference structure comprising four conventional InAs QD layers separated by a 50-nm-thick GaAs layer.

We fabricated a SOA device structure by processing a mesa structure and forming insulation films (comprising SiO_2 and benzocyclobutene), a protection film containing SiN, electrodes, and high-reflection coating with reflectivity of 83% for the front side and 97% for the back side. Owing to such high-reflection coating which enables us to characterize the net modal gain, the fabricated SOA device structure is identical to a laser device. The ridge width and the device length were 11 and 1000 μm, respectively. The waveguide directions were [−110] and [110].

The crystallographic properties of the stacked QDs were examined using a cross-sectional transmission electron microscope (TEM). Figures 1(a) and 1(b) show TEM images obtained from the [−110] and [110] directions, respectively. The SLN used in the TEM observation was 20. The wetting layer interfaces are very clear, and well-aligned stacking of QDs was confirmed. Moreover, the lateral QD dimension

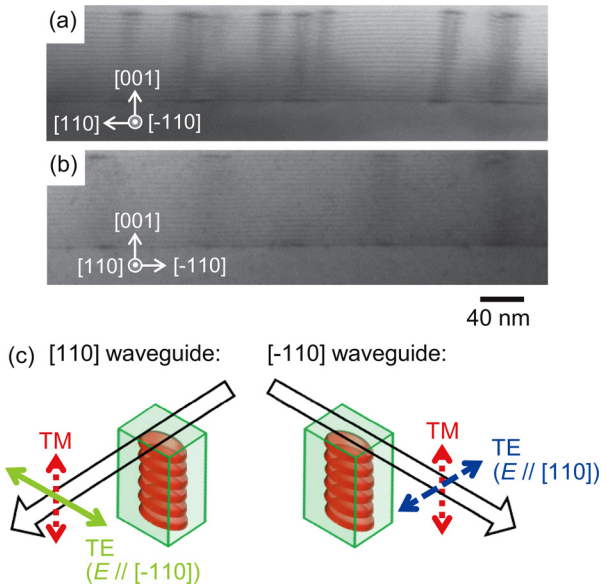

FIG. 1. (a) (−110) and (b) (110) cross-sectional TEM images of the 20-stacked InAs/GaAs QDs. (c) Schematic illustration of stacked QDs in [110]- and [−110]-waveguide directions.

does not shows a significant change with stacking as reported in Ref. 19. According to these results, the average lateral dimensions are 20 nm along [110] and 30 nm along [−110]. The QD density was approximately $1.0 \times 10^{10}\,\mathrm{cm}^{-2}$. Configurations of stacked QDs with the asymmetric dimensions in the waveguide directions are illustrated in Fig. 1(c).

III. POLARIZED ELECTROLUMINESCENCE

Electroluminescence (EL) measurements were performed at 21 °C; the temperature was controlled using a Peltier device. The EL signal was dispersed by a 30-cm single monochromator and was detected by a liquid-nitrogen-cooled InGaAs-diode array. Figure 2 shows linearly polarized EL spectra of 30- and 40-stacked QD devices as well as the reference device including InAs QD layers separated by 50-nm-thick GaAs. The injection current density was $100\,\mathrm{A/cm}^2$.

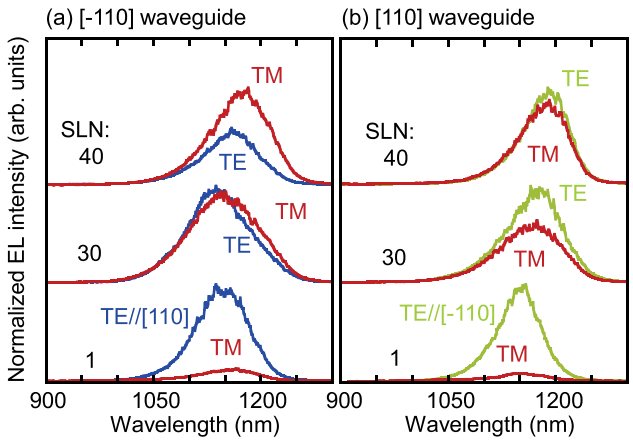

FIG. 2. Linearly polarized EL spectra of 30- and 40-stacked QD devices as well as the reference device with (a) the [−110] and (b) [110] waveguides. The device temperature was controlled at 21 °C using a Peltier device. The injection current density was $100\,\mathrm{A/cm}^2$.

The EL-peak wavelength appeared in between 1150 and 1200 nm, which shows a gradual shift with the stacking because of the increase in the volume of the stacked QDs. Moreover, the spectral line width of the stacked QD devices was broader than that of the reference device. The line width of 30-stacked QDs in the [−110] ([110]) waveguide was approximately 100 (94) and 106 (103) nm for TE and TM, respectively. These are larger than the TE-band width of 80 (65) nm for conventional InAs QDs capped with a thick GaAs layer in the [−110] ([110]) waveguide. The spectral broadening in stacked QDs arises from distributions of the lateral dimension[15] and the strain field[14] along the stacking direction. With stacking further, the line width tends to become narrow as observed for 40-stacked QDs. This suggests that transport of excited carriers in the miniband toward stable lower energy states in the fluctuating potential along the stacking direction. The line width of the device with the [−110] waveguide is broad rather than that of the [110] waveguide. According to the cross-sectional TEM images in Figs. 1(a) and 1(b), the relatively small lateral dimension along [110] causes a rather stronger confinement of QDs. Thus, the influence of the lateral dimension fluctuation on the quantized states becomes sensitive in the [−110] waveguide, which leads the relatively large broadening. On the other hand, the line width of the TM band of stacked QDs is slightly wider than that of the TE band. This reflects the anisotropic distribution of the electronic states for TE and TM.

The conventional QD shows obvious TE dominance polarized in the (001) plane, and its polarization anisotropy is independent of the waveguide direction. The TM polarization component (red line) is dramatically enhanced for the device with the highly stacked QDs. The [−110] waveguide almost exhibits polarization isotropy between the TE and TM components for the 30 stacked QDs and finally exhibits TM dominance for the 40 stacked QDs. On the other hand, the [110] waveguide shows an almost isotropic feature for the 40 stacked QDs.

These results are consistent with our previous theoretical predictions discussed in Ref. 13; i.e., polarization isotropy between TE//[−110] and TM//[001] occurs for a taller QD. It is noted that a remarkable anisotropy between the [−110] and [110] polarizations appears in the highly stacked, tall QDs because of the valence band mixing of the heavy- and light-hole states caused by relaxing the vertical confinement. The polarization anisotropy is determined by the in-plane shape anisotropy of QDs as shown in Fig. 1. Then, the optical transition strength of the [−110]- and [110]-polarization components can be continuously changed by controlling the QD height.[13–15] The average lateral dimensions of 20 nm along [110] and 30 nm along [−110] drive up the optical transition strength for the [−110] component rather than the [110] one. On the other hand, the TM component polarized along the [001] monotonically increases with the stacking. According to these changes of the TE- and TM-transition strengths as a function of the stacking, two heights of the stacked QDs yield polarization isotropy: the isotropy for the [001] and [110] polarizations is satisfied at a relatively low stacking, and the isotropy for the [001] and [−110] polarizations appears when the height becomes taller. The transition strengths at these points showing the isotropy are different. The [−110] polarization becomes isotropic with the [001] component at a higher oscillator strength than that of the [110] polarization. These results predict that a higher isotropic optical gain between TE (E//[−110]) and TM (E//[001]) can be realized by using a taller QD.

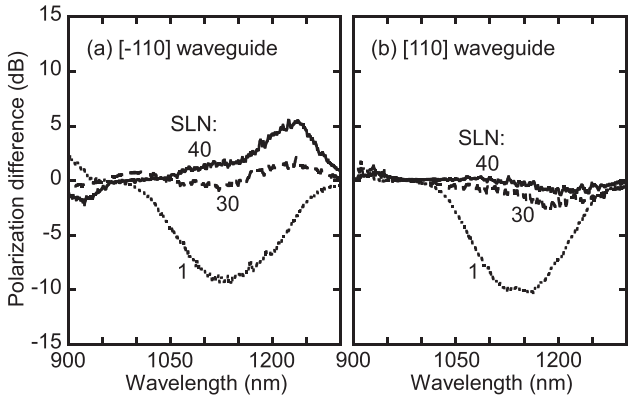

FIG. 3. PD spectra, defined by $10\log(I_{TM}/I_{TE})$, of 30- and 40-stacked QD devices as well as the reference device with (a) the [−110] and (b) [110] waveguides. I_{TM} and I_{TE} are the EL intensities with the TM- and TE-polarized components, respectively. The injection current density was 100 A/cm^2.

The polarization difference (PD) spectra defined by $10\log(I_{TM}/I_{TE})$ for these results are summarized in Fig. 3. Here, I_{TM} and I_{TE} are the EL intensities with the TM- and TE-polarized components, respectively. The PD within a few dB was confirmed for the 30 stacked QDs in the [−110] waveguide and the 40 stacked QDs in the [110] waveguide. The spectral bandwidth behaving such isotropy widely extends over almost the entire EL region greater than 150 nm.

IV. POLARIZED GAIN CHARACTERISTICS

The net modal gain spectrum was evaluated by analyzing the Fabry-Pérot oscillatory resonance features that appeared in a high-resolution EL spectrum obtained using the well-known Hakki-Paoli method,[20] which is a standard method for evaluating the net modal gain of a laser device operating below the threshold current. We can obtain the gain spectrum by analyzing the details of the Fabry-Pérot resonance appearing in the emission spectrum observed from a waveguide. The net modal gain g is given by the following equation:

$$g = \frac{1}{L}\ln\left(\frac{\gamma^{\frac{1}{2}}-1}{\gamma^{\frac{1}{2}}+1}\right) + \frac{1}{L}\ln\left(\frac{1}{R}\right), \quad (1)$$

where L is the cavity length, R is the averaged reflectivity, and γ is the ratio of the intensity maximum to the minimum of the Fabry-Pérot resonance. Figures 4(a) and 4(b) display the results for 30 stacked QDs: the Fabry-Pérot resonance as well as the analyzed gain and its PD, defined by $10\log(g_{TM}/g_{TE})$, obtained with injection current densities of 400 and 800 A/cm^2. g_{TM} and g_{TE} are polarized net modal gains evaluated using Eq. (1).

As the injection current increases, the EL intensity of the excited states increases on the shorter wavelength side,

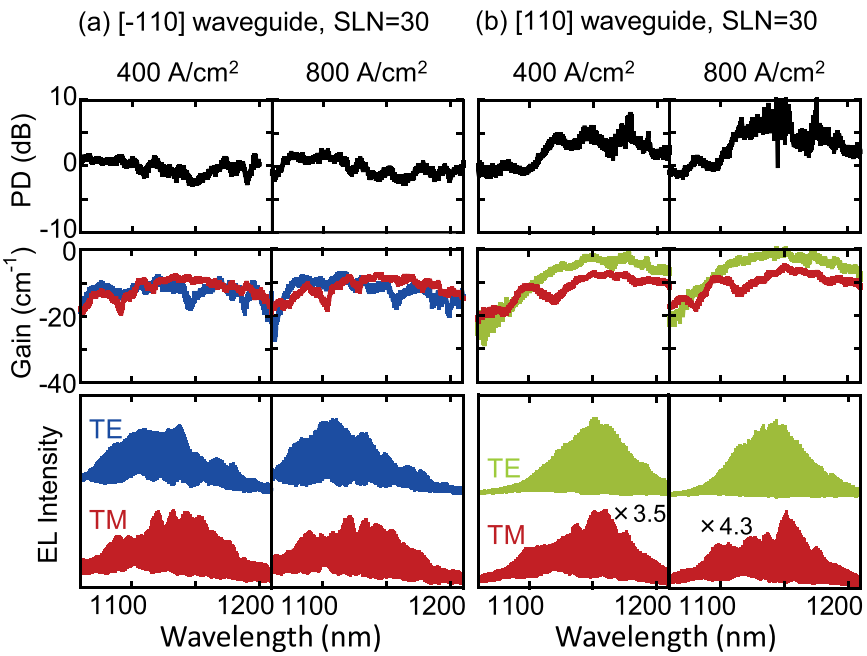

FIG. 4. Fabry-Pérot resonance, analyzed gain, and its PD, defined by $10\log(g_{TM}/g_{TE})$, obtained at 21 °C under the injection current density of 400 and 800 A/cm^2 for (a) the [−110]- and (b) [110]-waveguide device containing 30-stacked QD.

and, therefore, the gain becomes large. This trend is significant for the TE component. The PD amplitude of the [−110] waveguide is distributed within a few dB, even when the injection current increases. Conversely, the TE gain (green line) of the [110] waveguide becomes larger than that of the [−110] waveguide (blue line), although the TM gain (red line) was almost identical between the two waveguides. This causes the PD amplitude to increase toward the positive side, that is, the TE-dominant side. This feature indicates that the transition strength of the [−110]-polarization component is larger than that of the [110]-polarization component. For the [110] waveguide, with increasing injection current, the TE gain increases rapidly and approaches zero. Then, it exhibits laser oscillation. Thereby, in such conditions, the PD increases abruptly toward the positive side.

Similar phenomena have been observed for 40 stacked QDs. The results are displayed in Fig. 5. The [−110] waveguide with 40 stacked QDs shows a much smaller PD in the broad spectral range than that with 30 stacked QDs. This is due to the strong TM gain. In spite of the remarkable dominance of the TM-polarized EL for the [−110] waveguide with 40 stacked QDs, as shown in Fig. 2(a), the gain is almost isotropic. Such restriction of the enhancement of the TM gain arises from the anisotropic waveguide loss α and confinement factor Γ. The net modal gain g is defined by $g_m\Gamma - \alpha$, where g_m is the material gain of the stacked QDs, and α is the waveguide loss. Calculated Γ values for the TE and TM of our device structure were 0.715 and 0.704 at 1150 nm, respectively. Γ of the TM mode is smaller than that of TE. However, this anisotropy is too small to interpret the isotropy observed in the net modal gain. Therefore, the restriction of the enhancement of the TM gain is dominantly caused by an anisotropic loss, in particular internal absorption, in the waveguide structure.

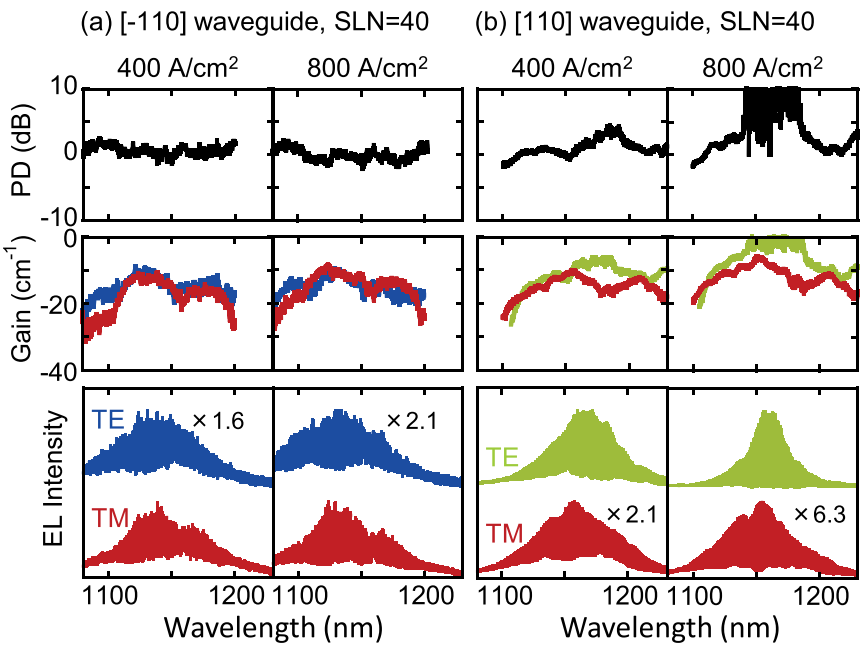

FIG. 5. Fabry-Pérot resonance, analyzed gain, and its PD, defined by $10\log(g_{TM}/g_{TE})$, obtained at 21 °C under the injection current density of 400 and 800 A/cm^2 for (a) the [−110]- and (b) [110]-waveguide device containing 40-stacked QD.

The PD amplitude of the [110] waveguide with 40 stacked QDs (Fig. 5(b)) at an injection current of 400 A/cm^2 was within 3 dB, which is smaller than that of the waveguide along the same direction with 30 stacked QDs (Fig. 5(b)). Comparing Figs. 4(a) and 5(b) in the sub-threshold gain region, we find that the PD of the [110] waveguide with 40 stacked QDs is nearly identical to that of the [−110] waveguide with 30 stacked QDs. Besides, the maximum gain of the [110] waveguide with 40 stacked QDs is larger than that of the [−110] waveguide with 30 stacked QDs. This result demonstrates that the high gain isotropy of the [110] waveguide occurs for taller QDs than that of the [−110] waveguide. With increasing the injection current for the [110] waveguide with 40 stacked QDs, the TE gain also shows a drastic increase and exhibits laser oscillation of the TE mode. Furthermore, a much higher injection current, over 800 A/cm^2, yielded both TE- and TM-mode lasing. Here, we note that the gain spectra of TE and TM contain multiple peaks, and the peak position depends on the polarization. The peaks appeared at the shorter wavelength side are attributed to the excited states. We confirmed that a clear difference between the gain spectra of the [110]- and [−110]-polarized TE, whereas the feature of the TM gain spectrum was almost the same. In particular for the [110] waveguide, the laser oscillation of TE (E//[−110]) at the excited states easily occurs,[21] and, therefore, the gain increases at the excited states, which takes over the gain spectrum.

Finally, we discuss the stacking layer number achieving a strong TM polarization. The QD heights of the 30 and 40 stacked QD are approximately 120 and 160 nm, respectively. For taller, highly stacked QDs, the biaxial strain at the center portion of the height approaches zero and tends to change toward biaxial tensile because of the strong vertical uniaxial compression.[8,14] This biaxial tensile strain at the center portion lifts the light-hole component and increases heavy-hole and light-hole mixing, which plays a large role in enhancing the TM gain. Thus, the height reflecting on the isotropic optical properties is smaller than that of the actual height. Moreover, our recent study regarding the superlattice formation of highly stacked InAs/GaAs QDs demonstrated that SLN greater than 20, corresponding to ∼80-nm height, is essential to cause obvious one-dimensional translational motion of carriers.[15] For small QD height, wave functions tend to localize near the base, particularly at elevated temperatures at which thermally populated carriers move toward the base side, which has a lower potential.[15] Thus, highly stacked QDs enhancing the TM gain at room temperature can be formed when the SLN is greater than 20. Besides, according to our recent atomistic theoretical study for the polarization response of highly stacked InAs/GaAs QDs, more than 6 SLN is necessary for achieving an isotropy between TE (E//[110]) and TM (E//[001]). Thus, it is convincing that the isotropy was observed when stacking approximately 30 layers.

V. SUMMARY

The polarized optical gain characteristics of highly stacked InAs/GaAs QDs with a thin spacer layer were studied in the sub-threshold gain region. Electronic coupling along the stacking direction was realized using a 4.0-nm-thick spacer layer. According to theoretical predictions obtained using a simple cubic model with an in-plane shape anisotropy of QDs, the [−110] polarization becomes isotropic with the [001] component at a higher oscillator strength than that of the [110] polarization. We systematically studied polarized EL properties of laser devises containing 30 and 40 stacked InAs/GaAs QDs. The net modal gain was analyzed using the Hakki-Paoli method. The gain showing polarization isotropy is high for the [110] waveguide structure, which occurs for 40 stacked QDs. Conversely, isotropic gain of the [−110] waveguide was achieved even for 30 stacked QDs. These results of the isotropy of the net modal gain are the fundamentals of designing the chip gain, defined by $G = \exp(gL)$ where L is a waveguide length, of a SOA device.

ACKNOWLEDGMENTS

We deeply thank Dr. M. Ekawa of Fujitsu Laboratories Ltd. for processing devices used in this work and Professor H. Yasuda and Dr. E. Taguchi of Osaka University for supporting our TEM observations. This work was partially supported by a Grant-in-Aid for Scientific Research (No. 24360121) from the Ministry of Education, Culture, Sports, Science and Technology, Japan.

[1]T. Kamiya and M. Tsuchiya, Jpn. J. Appl. Phys., Part 1 **44**, 5875 (2005).
[2]B. I. Miller, U. Koren, M. A. Newkirk, M. G. Young, R. M. Jopson, R. M. Derosier, and M. D. Chien, IEEE Photon. Technol. Lett. **5**, 520 (1993).
[3]M. Sugawara, N. Hatori, M. Ishida, H. Ebe, Y. Arakawa, T. Akiyama, K. Otsubo, T. Yamamoto, and Y. Nakata, J. Phys. D: Appl. Phys. **38**, 2126 (2005).
[4]M. Sugawara, H. Ebe, N. Hatori, M. Ishida, Y. Arakawa, T. Akiyama, K. Otsubo, and Y. Nakata, Phys. Rev. B **69**, 235332 (2004).
[5]P. Jayavel, H. Tanaka, T. Kita, O. Wada, H. Ebe, M. Sugawara, J. Tatebayashi, Y. Arakawa, Y. Nakata, and T. Akiyama, Appl. Phys. Lett. **84**, 1820 (2004).
[6]T. Kita, O. Wada, H. Ebe, Y. Nakata, and M. Sugawara, Jpn. J. Appl. Phys., Part 2 **41**, L1143 (2002).
[7]T. Kita, N. Tamura, O. Wada, M. Sugawara, Y. Nakata, H. Ebe, and Y. Arakawa, Appl. Phys. Lett. **88**, 211106 (2006).
[8]T. Saito, H. Ebe, Y. Arakawa, T. Kakitsuka, and M. Sugawara, Phys. Rev. B **77**, 195318 (2008).
[9]N. Yasuoka, K. Kawaguchi, H. Ebe, T. Akiyama, M. Ekawa, S. Tanaka, K. Morito, A. Uetake, M. Sugawara, and Y. Arakawa, Appl. Phys. Lett. **92**, 101108 (2008).
[10]K. Kawaguchi, N. Yasuoka, M. Ekawa, H. Ebe, T. Akiyama, M. Sugawara, and Y. Arakawa, Appl. Phys. Lett. **93**, 121908 (2008).
[11]P. Podemski, G. Sęk, K. Ryczko, J. Misiewicz, S. Hein, S. Höfling, A. Forchel, and G. Patriarche, Appl. Phys. Lett. **93**, 171910 (2008).
[12]T. Inoue, M. Asada, N. Yasuoka, O. Kojima, T. Kita, and O. Wada, Appl. Phys. Lett. **96**, 211906 (2010).
[13]Y. Ikeuchi, T. Inoue, M. Asada, Y. Harada, T. Kita, E. Taguchi, and H. Yasuda, Appl. Phys. Express **4**, 062001 (2011).
[14]M. Usman, T. Inoue, Y. Harada, G. Klimeck, and T. Kita, Phys. Rev. B **84**, 115321 (2011).
[15]A. Takahashi, T. Ueda, Y. Bessho, Y. Harada, T. Kita, E. Taguchi, and H. Yasuda, Phys. Rev. B **87**, 235323 (2013).
[16]K. Akahane, N. Ohtani, Y. Okada, and M. Kawabe, J. Cryst. Growth **245**, 31 (2002).
[17]O. Kojima, H. Nakatani, T. Kita, O. Wada, K. Akahane, and M. Tsuchiya, J. Appl. Phys. **103**, 113504 (2008).
[18]T. Kotani, P. Lugli, and C. Hamaguchi, Appl. Phys. Lett. **103**, 031110 (2013).
[19]Z. R. Wasilewski, S. Fafard, and J. P. McCaffrey, J. Cryst. Growth **201–202**, 1131 (1999).
[20]B. W. Hakki and T. L. Paoli, J. Appl. Phys. **46**, 1299 (1975).
[21]J. Tatebayashi, N. Hatori, M. Ishida, H. Ebe, M. Sugawara, Y. Arakawa, H. Sudo, and A. Kuramata, Appl. Phys. Lett. **86**, 053107 (2005).